Distinct effects on gene expression of chemical and genetic manipulation of the cancer epigenome revealed by a multimodality approach

David Gius,[1,5] Hengmi Cui,[4,5] C. Matthew Bradbury,[1] John Cook,[2] DeeDee K. Smart,[1] Shuping Zhao,[1] Lynn Young,[3] Sheri A. Brandenburg,[4] Yali Hu,[4,6] Kheem S. Bisht,[1] Allen S. Ho,[1] David Mattson,[1] Lunching Sun,[1] Peter J. Munson,[3] Eric Y. Chuang,[1] James B. Mitchell,[2] and Andrew P. Feinberg[4,*]

[1]Radiation Oncology Branch, Radiation Oncology Sciences Program, Center for Cancer Research, National Cancer Institute
[2]Radiation Biology Branch, Center for Cancer Research, National Cancer Institute
[3]Mathematical and Statistical Computing Laboratory, Center for Information Technology, National Institutes of Health, Bethesda, Maryland 20892
[4]Institute of Genetic Medicine and Departments of Medicine, Molecular Biology, and Genetics, and Oncology Center, Johns Hopkins University School of Medicine, Baltimore, Maryland 21205
[5]These authors contributed equally to this work.
[6]Present address: Drum Tower Hospital, Nanjing University Medical School, China
*Correspondence: afeinberg@jhu.edu

Summary

We tested the hypothesis that the effects on gene expression of altered DNA methylation by 5-aza-2′-deoxycytidine (5-aza-CdR) and genetic (*DNMT* knockout) manipulation of DNA are similar, and distinct from Trichostatin A (TSA)-induced chromatin decondensation. Surprisingly, the effects of 5-aza-CdR were more similar to those of TSA than to *DNMT1*, *DNMT3B*, or double *DNMT* somatic cell knockout. Furthermore, the effects of 5-aza-CdR were similar at one and five days exposure, suggesting active demethylation or direct influence of both drugs on the stability of methylation and/or chromatin marks. Agents that induce gene activation through hypomethylation may have unintended consequences, since nearly as many genes were downregulated as upregulated after demethylation. In addition, a 75 kb cluster of metallothionein genes was coordinately regulated.

Introduction

Since the initial discovery of altered methylation in human cancer (Feinberg and Vogelstein, 1983), a host of epigenetic alterations have been found, including global hypomethylation, gene hypomethylation and hypermethylation, and loss of imprinting (Goelz et al., 1985; Feinberg and Tycko, 2004). Hypermethylation of the promoters of tumor suppressor genes was first observed in retinoblastoma (Greger et al., 1989; Sakai et al., 1991) and associated with their silencing (Ohtani-Fujita et al., 1993). Silencing with hypermethylation has been found in many other genes since, and gene activation and chromosomal instability have been associated with hypomethylation (Feinberg and Tycko, 2004). While methylation itself may be one mechanism for altered gene expression, other plausible processes include alterations in chromatin structure resulting in altered gene activity (Schmid et al., 1984; Lengauer et al., 1998; Tamaru and Selker, 2001).

The chemical agents used to modulate the expression of individual genes in most experimental studies of the cancer epigenome have been either 5-aza-CdR, an inhibitor of DNA methylation, or TSA, an inhibitor of histone deacetylation (Egger et al., 2004). However, the agents used in such studies may target one methyltransferase or chromatin compaction preferentially over another and exhibit nonspecific pharmacological effects on gene expression. Thus, a genetic approach to inhibit specific methyltransferases may represent a more rigorous experimental methodology.

It appears that methylation patterns in mammalian cells are regulated via a complex interplay of at least three independently encoded DNA methyltransferases (*DNMTs*): *DNMT1*, *DNMT3A*, and *DNMT3B* (Bestor, 2000; Robertson, 2001; Rhee et al., 2002).

SIGNIFICANCE

Most experimental studies of the cancer epigenome have employed 5-aza-CdR, an inhibitor of DNA methylation that is presumed to be specific. Other studies have used TSA that inhibits histone deacetylase and subsequently alters chromatin compaction. Still other recent studies have employed a genetic approach, using single and double somatic cell knockouts of DNA methyltransferases 1 and 3B. To our knowledge, however, pharmacological and genetic manipulations have not been performed within the same context to date, preventing the precise definition of their shared or distinctive effects on gene expression. A multimodality experimental approach combined with a comprehensive expression analysis should reveal the relationship between chemical and genetic manipulation of the epigenome, as well as unexpected relationships among the gene targets themselves.

Somatic knockout cell lines for methyltransferase (*DNMT1*$^{-/-}$, *DNMT3B*$^{-/-}$, and double knockouts [DKO]) have been constructed previously (Rhee et al., 2002) and represent an ideal model system to investigate the epigenetic regulation of gene expression. It has previously been shown that *DNMT1* and *DNMT3B* cooperatively maintain DNA methylation and gene silencing (Rhee et al., 2002), and genetic disruption of both *DNMT1* and *DNMT3B* significantly inhibited methyltransferase activity and reduced genomic DNA methylation by roughly 95% (Rhee et al., 2000, 2002). In contrast, a single knockout of *DNMT1* exhibited markedly decreased cellular DNA methyltransferase activity with only modest global effects on methylation (20%) (Rhee et al., 2000). Others, using *DNMT1*$^{-/-}$ mouse fibroblasts, demonstrated significant changes in gene expression patterns (>5%) when only a single methyltransferase was disrupted (Jackson-Grusby et al., 2001). Although these are different systems, the results of these studies together suggest that the change in gene expression may not reflect the degree of change in global methylation.

Determination of the relationship between DNA methylation and global changes in gene expression has not been previously addressed in a comprehensive manner. In one study, methylation was examined using differential methylation hybridization (DMH) and amplification of intermethylated sites (AMS) combined with a 34 gene CpG island microarray (Paz et al., 2003). However, a microarray-based gene expression analysis and the effects of 5-aza-CdR and TSA were not within the scope of that study. To date, the only microarray-based approach to examine the regulation of the epigenome used RKO colon carcinoma cells treated with 5-aza-CdR followed by cDNA subtraction (Suzuki et al., 2002). However, in this study, no comparison to *DNMT* knockout cells was done.

In the present study, we chose a combined approach employing pharmacological and/or genetic manipulation to examine the expression of a large number of genes. A rigorous statistical analysis of microarrays was performed on HCT116, *DNMT1*$^{-/-}$, *DNMT3B*$^{-/-}$, and DKO cell lines, with and without exposure to 5-aza-CdR, TSA, or both. This work was designed to significantly expand upon previous studies referenced earlier (Jackson-Grusby et al., 2001; Suzuki et al., 2002; Paz et al., 2003). To generate data that were statistically significant, valid, and reproducible, experiments were repeated in triplicate with at least two microarrays per sample on nearly 8000 genes, resulting in greater than 100 microarrays in total. The data were analyzed in the context of existing knowledge about gene expression regulation by methylation status and methyltransferase activity to uncover previously unknown relationships.

Results

A gene expression clustering analysis algorithm applied to the epigenome

A hierarchical gene-based clustering algorithm was employed, and sufficient statistical power was attained using multiple subclones, RNA collections, and microarray hybridizations for each somatic knockout cell line. Accordingly, at least four RNA samples per cell line and up to eight microarrays were used to account for any potential clonal differences or RNA collection variability (see Supplemental Table S1 at http://www.cancercell.org/cgi/content/full/6/4/361/DC1/), with or without experimental treatment with 5-aza-CdR or TSA. Genes were evaluated if they met a union of conditions: (1) they showed statistically significant differences using a Mann-Whitney U-Test ($p < 0.05$, not corrected for multiplicity), and (2) they exhibited a minimum 1.5-fold difference in expression, relative to control. Three additional analysis methods were employed to validate statistical integrity: class comparison, class prediction, and false discovery, all performed at $p = 0.05$ (see Supplemental Tables S2 and S3). The resulting expression ratios were displayed relative to each other using a hierarchical clustering algorithm to indicate up- or down-regulation (red: ≥1.5-fold upregulated; green: ≥1.5-fold downregulated; black: no change). These results identify regions of differential response to pharmacological (Figure 1A) or genetic (Figure 1B) modification of methyltransferase activity.

The effects of 5-aza-CdR closely resembled those of TSA, with subtle differences

Previous experiments to determine the effects of 5-aza-CdR or TSA have focused on measurement of individual gene expression or have used microarray analysis with limited replication, restricting statistical robustness. We attempted to overcome these limitations by analyzing the microarray expression profile of HCT116 cells following their exposure to 5-aza-CdR and/or TSA. A hierarchical cluster map for HCT116 cells treated with 5-aza-CdR, TSA, or both, was constructed (Figure 1A).

Surprisingly, the responses of HCT116 cells to 5-aza-CdR (Figure 1A, column 3) and TSA treatment (Figure 1A, column 1) were very similar ($r\rho = 0.84$). In this case, $r\rho$ represents the Pearson's correlation coefficient, an approximation of similarity between two distinct data points where a value of 1.0 represents identical gene expression pattern (The black column left of column 1 represents control, untreated HCT116 cells). This high degree of similarity is clearly seen when comparing columns 1 and 3 in areas I–IV, where there is an especially high $r\rho$ value. This similarity is also seen when comparing concurrent treatment with both agents (column 2) to treatment with TSA or 5-aza-CdR alone.

Several examples of genes previously shown to be upregulated by exposure to either 5-aza-CdR or TSA include insulin-like growth factor 1 (*IGF1*), an autocrine growth factor (Furstenberger and Senn, 2002), platelet-derived growth factor-β (*PDGF-B*), which regulates pro-proliferative signaling pathways (Ulleras et al., 2001), and TRF-2 interacting telomeric RAP-1 protein (*RAP1*), implicated in a wide range of biological processes from cell proliferation, differentiation, and cell adhesion (Storks, 2003). These genes, as well as others altered by the addition of 5-aza-CdR and TSA, are shown (see Supplemental Table S4).

The analysis of HCT116 cells treated with chemical agents also identified several genes not previously shown to be regulated by chemical modification. These genes include pituitary tumor-transforming factor (*PTTG1*) and peroxiredoxin 2 and 3 (*PRDX*2 and *PRDX3*). Multiple CpG islands are contiguous to or immediately upstream of these genes (identified using Entrez Genome, National Center of Biotechnology Information). The results of these experiments suggest that the effects of 5-aza-CdR and TSA on gene expression are considerably more similar than previously demonstrated, suggesting a common upstream pathway leading to altered gene expression.

Chemical effects on gene expression patterns were independent of dose and duration of exposure

The results presented in Figure 1A represent a 24 hr exposure to 10 μM of 5-aza-CdR. To exclude the possibility that some

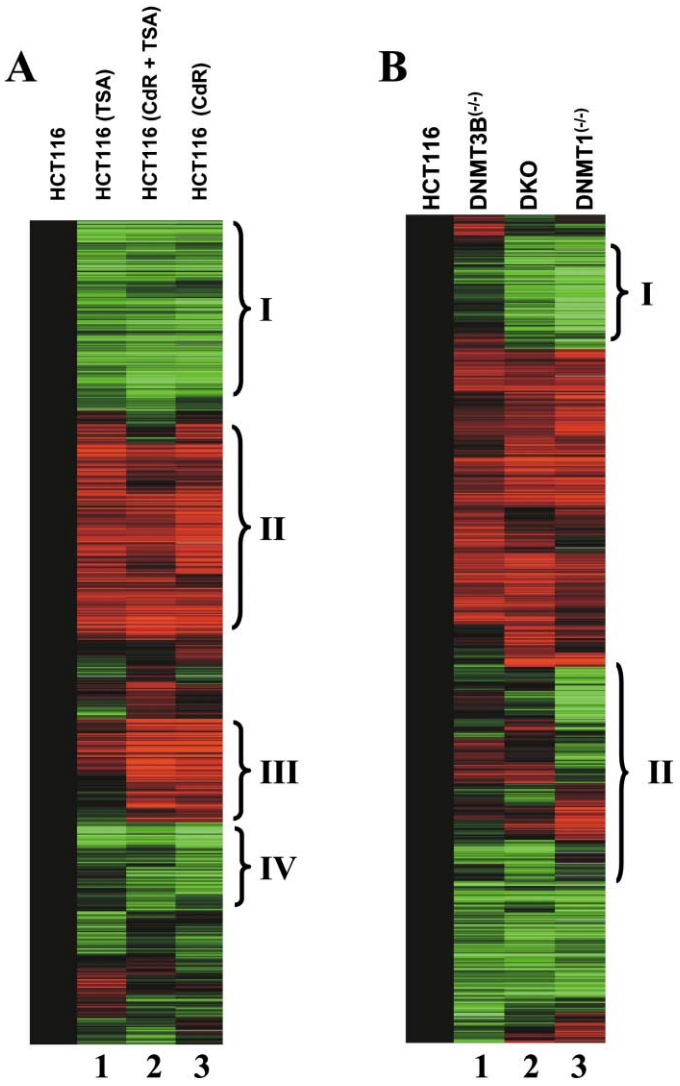

Figure 1. Hierarchical clustering of gene expression following pharmacological or genetic alteration of methyltransferase activity

A: Cluster map of HCT116 cells treated with 5-aza-CdR, TSA, or 5-aza-CdR concurrent with TSA for 24 hr. Mean gene expression values were determined from experimental replicates, calculated as a ratio of HCT116 expression, and clustered hierarchically using Cluster (v. 2.20) and TreeView (v. 1.60) software (Eisen and Brown, 1999). The left-most column represents the ratio of untreated HCT116 to itself and is therefore black (indicating no change). Column 1 represents the ratio of TSA-treated to untreated HCT116 cells, where red represents an increase in RNA message, green a decrease. Similar relationships were determined for the combination 5-aza-CdR and TSA (column 2) and the 5-aza-CdR treatment (column 3), relative to untreated HCT116 cells.

B: Gene expression of DNMT1$^{-/-}$, DNMT3B$^{-/-}$, and DKO cells, relative to parental HCT116 cells. Gene expression data were clustered as described above and displayed relative to untreated, parental HCT116 cells. Column 1 represents the expression ratio of DNMT3B$^{-/-}$ to HCT116, column 2 represents that of DKO to HCT116, and column 3 represents that of DNMT1$^{-/-}$ to HCT116.

of the changes in gene expression might be due to drug-induced cytotoxicity, HCT116 cells were also treated with a lower concentration (1 μM) of 5-aza-CdR, as well as for varying durations (both 1 and 5 days). Overall gene expression patterns at varying conditions were then compared using Pearson's correlation coefficient values. This analysis demonstrated surprisingly little variability in gene expression, comparing either time of exposure or concentration of 5-aza-CdR, with differences in correlation coefficients (rρ) between 0.95 and 0.99 (Table 1, upper panel). Thus, while 5-aza-CdR minimally decreases cell growth rates at one day and substantially at five days (see Supplemental Table S5 at http://www.cancercell.org/cgi/content/full/6/4/361/DC1/), very little difference in overall gene expression patterns is evident comparing concentration or duration (Table 1, upper panel). These results suggest that the global effects of 5-aza-CdR on gene expression patterns are remarkably similar and that nonspecific drug-induced toxicity is unlikely to account for a significant fraction of the changes in gene expression after 5-aza-CdR.

Table 1. Similarity of HCT116 and SW48 cells treated with 5-aza-CdR, TSA, or butyrate, as demonstrated by Pearson's correlation coefficient values (rρ)

		1 μM CdR		10 μM CdR		
HCT116		1d	5d	1d	5d	TSA
1 μM CdR	1d	—	—	0.983	0.998	0.761
	5d	0.998	—	0.966	0.971	0.726
10 μM CdR	1d			—	—	0.708
	5d			0.956	—	0.733
5 mM butyrate		0.947	0.912	0.863	0.856	0.541
		HCT116				
		1 μM CdR		10 μM CdR		
SW48		1d	5d	1d	5d	
1 μM CdR	1d	0.976	—	0.972	—	
	5d	—	0.970	—	0.971	
10 μM CdR	1d	0.977	—	0.974	—	
	5d	—	0.962	—	0.911	

Pearson's correlation coefficient (rρ), an approximation of similarity between two distinct data points, where a value of 1.0 represents identical gene expression pattern.

Likewise, HCT116 cells were treated with sodium butyrate, an alternative to TSA for inhibition of histone deacetylation, and evaluated for similarity in gene expression patterns. Treatment with 5 mM of butyrate showed a strong similarity to that of HCT116 cells treated with 5-aza-CdR, with resulting Pearson's correlation coefficient values between 0.947 and 0.856, depending on concentration and time (Table 1, upper panel). The rρ value of butyrate compared to TSA was 0.541 (Table 1, upper panel). As an additional control, to rule out an idiosyncratic effect on HCT116 cells, we treated a second colon cancer cell line, SW48, with 5-aza-CdR, at both 1 and 10 μM concentrations, and for both 1 and 5 days. The effect on gene expression patterns was again nearly identical between the two colon cancer cell lines, with rρ values between 0.91 and 0.97 resulting from comparison of 5-aza-CdR treatments (Table 1, lower panel).

Silencing of genes by 5-aza-CdR or TSA

Since methylation acts to inhibit gene expression, and demethylating agents are believed to behave as negative regulators and expression activators, most studies have examined only genes that are upregulated following exposure to 5-aza-CdR and/or TSA. However, this study identified several genes that are downregulated following exposure to 5-aza-CdR and/or TSA, suggesting that methylation increases gene expression either indirectly or directly. A hierarchical cluster analysis identified

Table 2. Similarity of somatic cell knockout cells to each other and to 5-aza-CdR-treated HCT116 cells, as demonstrated by Pearson's correlation coefficient values (rρ)

	DNMT1$^{-/-}$	DNMT3B$^{-/-}$	DKO
HCT116	0.22	0.63	0.32
DNMT1$^{-/-}$	—	0.42	0.76
DNMT3B$^{-/-}$	—	—	0.52
Knockout cell line	HCT116 5-aza-CdR	DNMT1$^{-/-}$ 0.71	DNMT3B$^{-/-}$ 0.42

Pearson's correlation coefficient (rρ), an approximation of similarity between two distinct data points, where a value of 1.0 represents identical gene expression pattern.

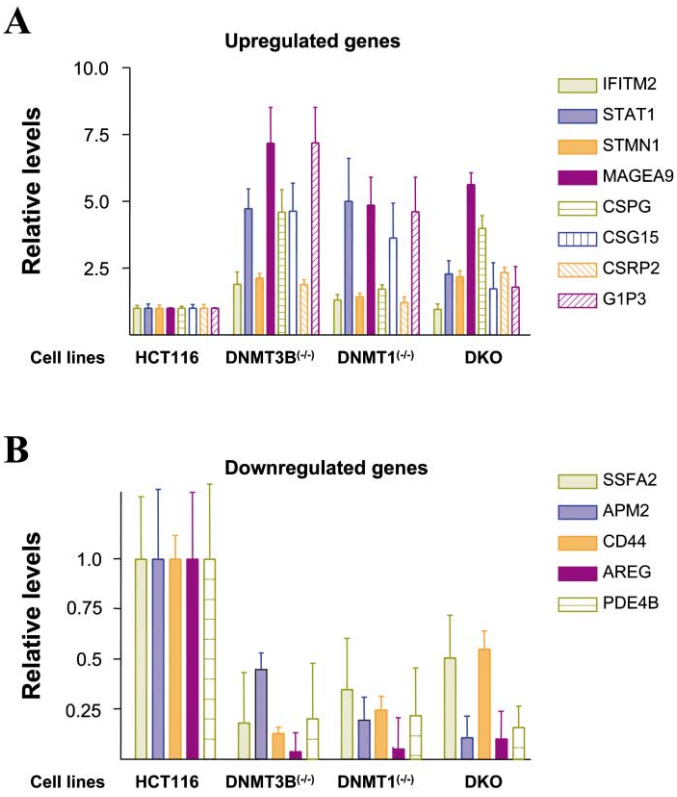

Figure 2. Real-time, RT-PCR verification of gene expression in parental and knockout cell lines

Validation of cDNA microarray data using the real-time, RT-PCR assay to establish expression ratios between HCT116, *DNMT1*$^{-/-}$, *DNMT3B*$^{-/-}$, and DKO cell lines. Upregulated genes (**A**) and downregulated genes (**B**) are shown. The total RNA used for the real-time, RT-PCR assay was taken from one set of the three replicate experiments, and the real-time, RT-PCR data shown represent the average of three independent reactions.

329 genes downregulated at least 1.5-fold by 5-aza-CdR, 154 genes by TSA, and 176 downregulated at least 1.5-fold following exposures to both agents. These genes include interleukin enhancer binding factor (*ILF3*), cyclin B2 (*CCNB2*), and cyclin 25B (*CDC25B*), c-myc binding protein (*MYCBP*), and hepatoma-derived growth factor (*HDGF*), none of which have been previously shown to have altered expression to 5-aza-CdR or TSA exposure. Upon examination, each of these genes was found to contain a CpG island overlapping the transcriptional start site (identified using Entrez Genome, NCBI). A complete list of genes downregulated by chemical modification of methylation is available (see Supplemental Table S6). Among these, ILF3 has been shown to interact with and is regulated by protein-arginine methyltransferase-1 (*PRMT1*), the predominant intracellular protein-arginine methyltransferase (Tang et al., 2000). The possible mechanism accounting for these results is unclear and may include either direct effects on CpG islands (e.g., insulator activity) or indirect nonspecific effects of the chemical agents. The results of these experiments suggest that chemical agents that inhibit methyltransferase activity or chromatin structure act both to increase and to decrease the expression of specific genes.

DNMT1$^{-/-}$ and DNMT3B$^{-/-}$ cell lines showed substantial differences in gene expression

To comprehensively address the effect of genetic inhibition of methyltransferase on gene expression, values from untreated somatic cell knockout lines for *DNMT1*$^{-/-}$, *DNMT3B*$^{-/-}$, and double knockouts (DKO) were analyzed. The data were clustered in both directions (i.e., by genes and by cell lines), and an initial analysis of the data clearly demonstrated distinct differences between the *DNMT1*$^{-/-}$, *DNMT3B*$^{-/-}$, and DKO cell lines. *DNMT3B*$^{-/-}$ cells showed the fewest changes in gene expression, relative to the parental HCT116 cells (Figure 1B). Examination of column 1 versus columns 2 and 3, in the areas designated I and II, clearly shows fewer differences in up- or downregulated genes in *DNMT3B*$^{-/-}$ than either *DNMT1*$^{-/-}$ or DKO cells, compared to HCT116 cells. This is also reflected in the Pearson's correlation coefficient value for HCT116 versus DNMT3B$^{-/-}$ (rρ = 0.63) (Table 2, upper panel), indicating a moderate similarity in gene expression patterns (see Supplemental Table S7 for raw values).

In contrast, *DNMT1*$^{-/-}$ cells showed the greatest number of genes with differential expression (HCT116 versus *DNMT1*$^{-/-}$, rρ = 0.22) (Table 2, upper panel). This is seen when comparing column 3 in the areas designated I and II with column 1 or 2 (Figure 1B). A complete analysis of gene expression patterns is available (see Supplemental Table S7). Curiously, DKO cells (column 2) showed an intermediate change in the gene expression pattern between those of either single knockout cell line (HCT116 versus DKO, rρ = 0.32) (Table 2, upper panel). This interpretation was confirmed by a pairwise comparison of each genotypes: *DNMT1*$^{-/-}$ versus *DNMT3B*$^{-/-}$ (rρ = 0.42); *DNMT1*$^{-/-}$ versus DKO (rρ = 0.76); and *DNMT3B*$^{-/-}$ versus DKO (rρ = 0.52) (Table 2, upper panel).

These results suggest that the effects of genetic disruption of *DNMT1* and *DNMT3B* on gene expression are not simply additive, but likely involve a complex interplay between the two pathways. These results may also resolve a controversy regarding the original observation of Rhee et al. (2002), who found residual methyltransferase activity in their *DNMT1* knockout cell line. In the course of our analysis, we observed a 3.1-fold increase in DNMT3B expression in DNMT1$^{-/-}$ cells, suggesting a potential compensatory upregulation of *DNMT3B* gene expression to offset the functional loss of *DNMT1*.

Validation of microarray data

To further confirm the results of microarray analysis, real-time, quantitative reverse transcription (RT) PCR analysis was conducted for 13 randomly selected genes from the HCT116,

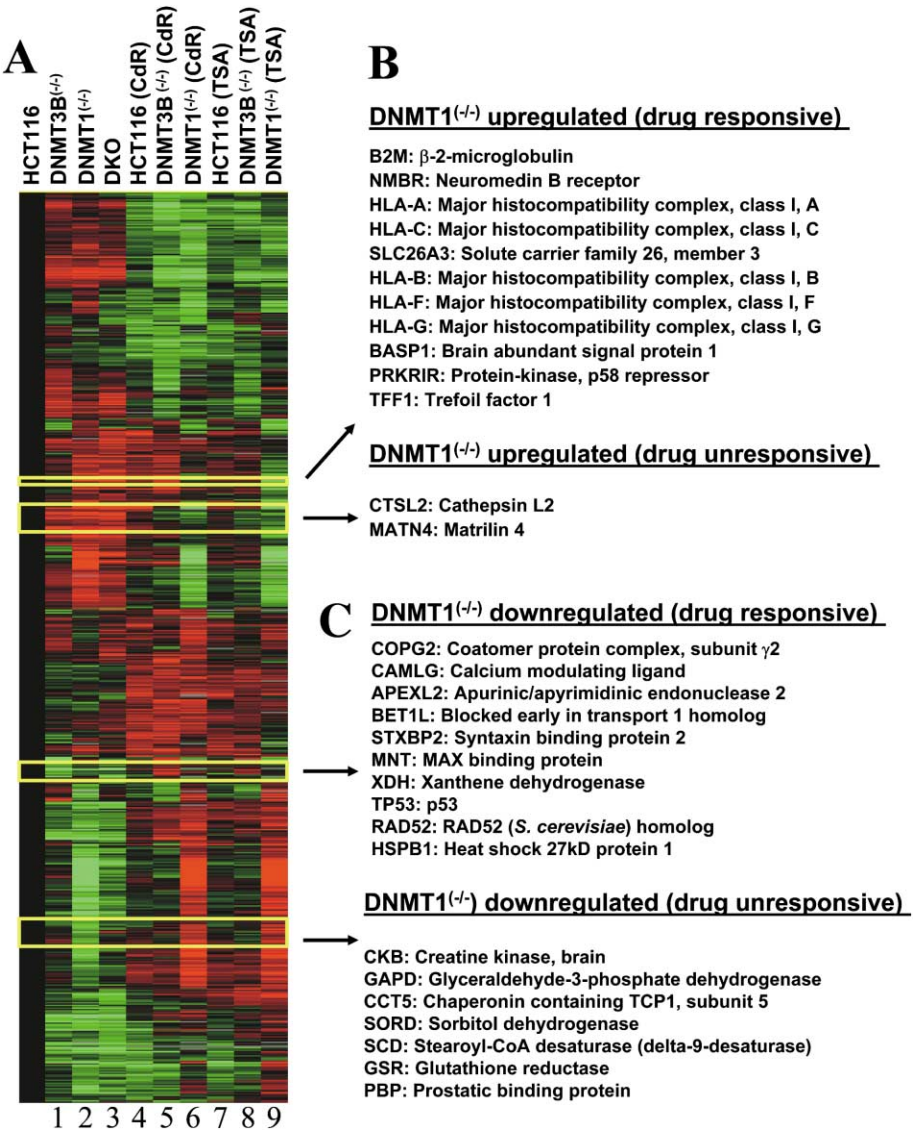

Figure 3. Hierarchical clustering of gene expression in *DNMT1*$^{-/-}$ knockout cells by pharmacological alteration with 5-aza-CdR and/or TSA

A: Ratios of gene expression values were generated and clustered hierarchically as described in Figure 1. Up- (i.e., red) and down- (i.e., green) regulation identified gene responsiveness to 5-aza-CdR and/or TSA treatment unique to the genetic knockouts. The black, left-most column represents control, HCT116 cells.

B and C: Yellow boxes denote boundaries of the clusters. **B:** Genes upregulated in the *DNMT1* knockout that are either drug-responsive or drug-unresponsive are shown. **C:** Genes downregulated in the DNMT1 knockout that are either drug-responsive or drug-unresponsive are shown. NCBI abbreviations and gene names shown in the respective clusters, as enclosed by yellow rectangles, are not inclusive of all genes within the cluster box.

DNMT1$^{-/-}$, *DNMT3B*$^{-/-}$, and DKO cell lines. The total RNA used for the RT-PCR experiments were taken from one set of the three replicate experiments, and the RT-PCR data shown represent the average of three independent reactions. Upregulated (Figure 2A) and downregulated (Figure 2B) genes are shown, as are the sequences of primers and probes used (see Supplemental Table S8). Comparison of the real-time, RT-PCR results showed a complete (100%) concurrence in terms of increases or decreases in gene expression with those measured using the microarray data, with no more than a 25% difference in relative values. Thus, results of the experiments in Figure 2 indicate an excellent agreement between the microarray and real-time, RT-PCR analyses.

Gene expression patterns after chemical and genetic inhibition of methyltransferase differed

In order to compare the effects on gene expression of chemical inhibition with genetic knockout of methyltransferase activity, a hierarchical cluster map of the *DNMT1*$^{-/-}$, *DNMT3B*$^{-/-}$, and DKO somatic cell lines versus the parent HCT116 cells was generated, as well as a similar map of the *DNMT1*$^{-/-}$, *DNMT3B*$^{-/-}$, and HCT116 somatic cell lines exposed to either 5-aza-CdR or TSA (Figure 3A). The DKO cells could not be treated with either 5-aza-CdR or TSA, due to cell death as early as 24 hr following start of treatment. Using Pearson's correlation, the pattern of gene expression in HCT116 cells treated with 5-aza-CdR more closely resembled that of the *DNMT1*$^{-/-}$ cells ($r\rho = 0.71$, Table 2, lower panel) than *DNMT3B*$^{-/-}$ cells ($r\rho = 0.42$, Table 2, lower panel). Thus, the DNMT1 knockout more closely approximates the effects of 5-aza-CdR on gene expression than does the *DNMT3B* knockout.

Based on this result, we grouped target genes into four distinct classifications: those genes (1) upregulated by methyltransferase knockout and by 5-aza-CdR and TSA; (2) upregulated by methyltransferase knockout but unaffected by 5-aza-CdR and TSA; (3) downregulated by methyltransferase knockout and by 5-aza-CdR and TSA; and (4) downregulated by methyltransferase knockout but unaffected by 5-aza-CdR and TSA (Figure 3B). Genes upregulated by both methyltransferase

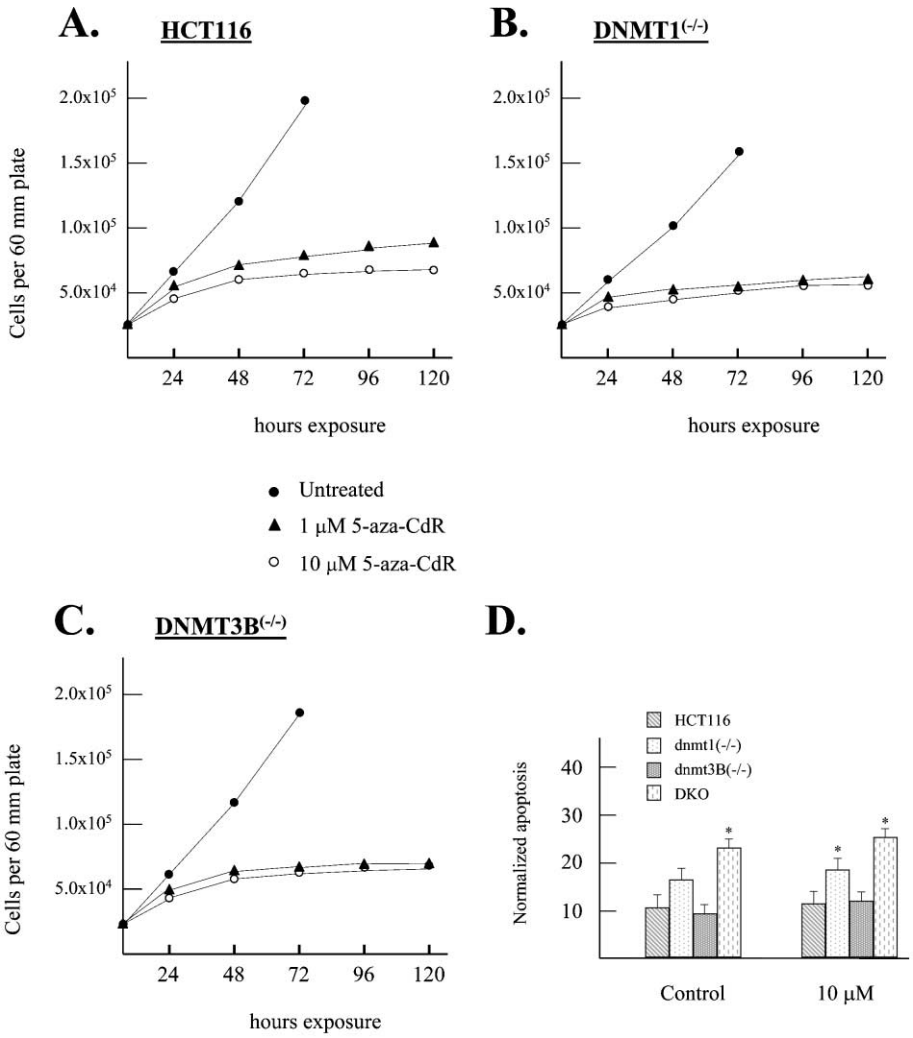

Figure 4. Cell growth rates and apoptosis in HCT116, *DNMT1*$^{-/-}$, *DNMT3B*$^{-/-}$, and DKO cell lines

A–C: HCT116 (**A**), *DNMT1*$^{-/-}$ (**B**), and *DNMT3B*$^{-/-}$ (**C**) cells were plated at 20,000 cells per 35 mm dish, treated continuously with 5-aza-CdR (1 or 10 μM), and subsequently counted at 1, 2, 3, 4, and 5 days to determine cell growth rates.

D: Results of Annexin V-FITC detection of apoptosis in HCT116, *DNMT1*$^{-/-}$, *DNMT3B*$^{-/-}$, and DKO following exposure to 10 μM of 5-aza-CdR. Cells were treated for 24 hr, and Annexin V-FITC was added to the cell suspension following incubated at room temperature for 15 min in dark. Samples were kept on ice in dark and analyzed by flow cytometry using Cell Quest and ModFit software. 10,000 events were collected for analysis. The asterisk identifies statistically significant differences ($p < 0.05$ by two-tailed Student's t test).

knockout and drug treatment included members of the major histocompatibility complex antigen (HLA) gene family, previously shown to be modulated by *DNMT1* (Nie et al., 2001; Guillaudeux et al., 1996). Several additional genes were found which clustered with the HLA genes; these include β-2-microglobulin (*B2M*), neuromedin B-receptor (*NMBR*), solute carrier family 26 (*SLC26A3*, a chloride pump), and trefoil factor 1 (*TFF1*). Of these, *SLC26A3* and *TFF1* are particularly interesting, given the recent report that a family member of *SLC26A3*, *SLC5A8*, has been identified as a tumor suppressor gene in colon cancer, and *TFF1* has been identified as a putative tumor suppressor gene with a methylated promoter in some gastric cancers (Carvalho et al., 2002). Genes upregulated by methyltransferase knockout but not by drug treatment included the bone development gene matrillin-4 (*MATN4*) and a member of the cathepsin gene family (CTSL2), which is involved in antigen processing. Complete lists of drug-responsive and -unresponsive genes are available for both *DNMT1*$^{-/-}$ and *DNMT3B*$^{-/-}$ (Figure 3B and see Supplemental Table S9).

5-aza-CdR effects on gene expression were independent of cell proliferation and apoptosis

Cellular proliferation rates and apoptosis were determined for the HCT116, *DNMT1*$^{-/-}$, and *DNMT3B*$^{-/-}$ cell lines after 5-aza-CdR exposure at 1 and 10 μM for 1 through 5 days. Proliferation assays (Figures 4A–4C) clearly showed that 5-aza-CdR decreases cell growth in all three cell lines, particularly at increasing times of exposure, and that the degree of growth delay is very similar among each cell line at identical concentrations (Figures 4A–4C). DKO cells were not tested, due to significant drug-induced cytotoxicity. Further experiments indicated that incidence of apoptosis was unchanged in the HCT116, *DNMT1*$^{-/-}$, and *DNMT3B*$^{-/-}$ cells following exposure to 10 μM of 5-aza-CdR (Figure 4D). Nevertheless, as described earlier, the pattern of gene expression after 5-aza-CdR was largely independent of dose and time of exposure. Therefore, the changes in gene expression are not secondary to changes in cell growth and apoptosis.

Hypomethylation of the APM2 promoter is associated with gene silencing

Previously, the loss of methylation of gene promoters with *increased* gene expression was demonstrated in DNMT somatic knockout cell lines (Rhee et al., 2002). One of the surprising results of the present study was the identification of a subset of genes whose gene expression was *decreased* by loss of methylation. In order to confirm an alteration in DNA methylation,

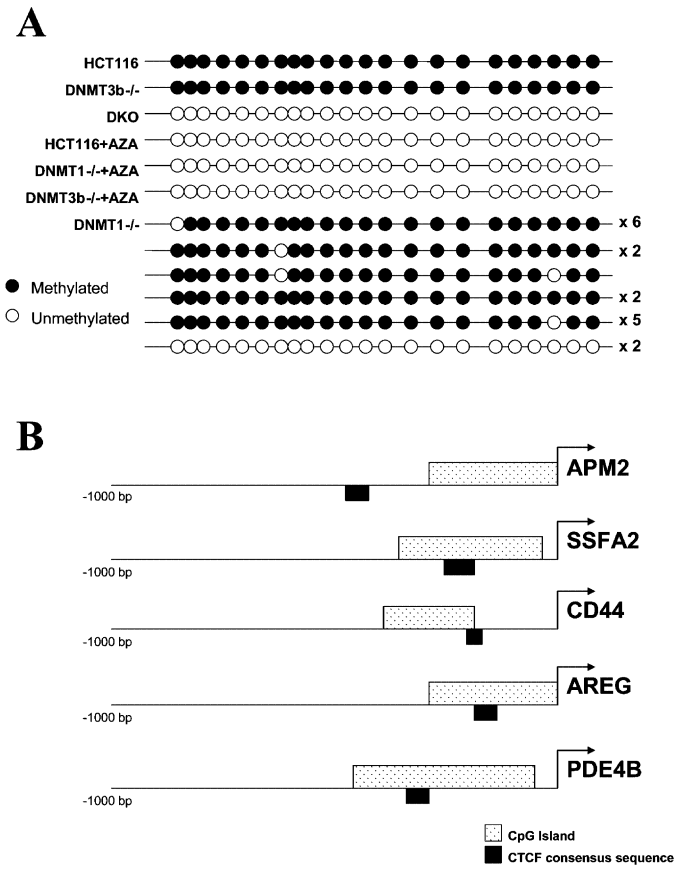

Figure 5. The *APM2* promoter CpG island is hypomethylated in somatic cell methyltransferase knockout cell lines

A: The methylation status of the CpG island in the *APM2* upstream promoter region was determined in HCT116, *DNMT1*$^{-/-}$, *DNMT3B*$^{-/-}$, and DKO cell lines as well as HCT116, *DNMT1*$^{-/-}$, and *DNMT3B*$^{-/-}$ treated with 5-aza-CdR for 24 hr.

B: The *APM2*, *SSFA2*, *CD44*, *AREF*, and *PDE4B* promoters were examined for the presence of CpG islands and CTCF binding sites using software available at Entrez Genome (http://ncbi.nlm.nih.gov) and the Genetics Computer Group (http://helix.nih.gov), respectively.

we examined the promoter region of *APM2*, which was shown to be silenced in the somatic knockout cell lines, and found that the degree of transcriptional silencing closely reflected the degree of hypomethylation observed in the *APM2* promoter (compare Figures 2B and 5A). Surprisingly, both the hypomethylation and the decrease in gene expression were observed at 24 hr of treatment with 5-aza-CdR (after 1–2 cell divisions at most), suggesting some form of active of active demethylation, rather than only passive demethylation, as might be expected.

It has been suggested that the CTCF insulator protein can block the transcriptional activity of enhancer elements (Bell et al., 1999; Bell and Felsenfeld, 2000; Hark et al., 2000, Holmgren et al., 2001), which could lead to hypomethylation-associated gene silencing. Consistent with this idea, all of the downregulated genes confirmed by real-time PCR (Figure 2B) contained a CpG island and at least one nearby consensus CTCF binding site (Figure 5B).

Metallothionein family genes constitute a cluster of differentially expressed genes

One of the purposes of this analysis was to determine whether methylation alterations could affect expression of clusters of genes, as suggested by recent studies of the effect of chromatin insulators on gene domains (Holmgren et al., 2001). To address this objective, a new analytical method was employed, which systematically searches the physical and genetic locations of differentially expressed genes for apparent clusters or groups of closely spaced, coregulated genes, and determines the statistical significance of such findings (as described in detail in the Experimental Procedures below and in the Supplemental Experimental Procedures at http://www.cancercell.org/cgi/content/full/6/4/361/DC1/). We uncovered one site of regional gene clustering, located at 16q13 (Figure 6A), and found five genes which were members of the same metallothionein (*MT*) gene family (Figure 6B, genes in bold). The other genes listed are either pseudogenes or not present on the microarray.

Several members of the metallothionein family have been previously shown to be regulated by methylation (Ghoshal et al., 2000; Majumder et al., 2002), and a regional analysis of methylation patterns in this segment of the genome clearly revealed the presence of multiple, strict (≥ 500 bp long, 50% or higher CG content) CpG islands (identified using Entrez Genome, NCBI; Figure 6B). However, several of the genes involved do not have a CpG island in the direct areas of either the open reading frame or the upstream regulatory region. These results suggest a novel mechanism involving methylation-induced regional chromosomal structural changes that alter the expression of a class of related genes colocalized to a specific chromosomal region.

Discussion

This study represents a comprehensive integrated experimental approach to the cancer epigenome, comparing the effects on gene expression of altered DNA methyltransferase activity due to genetic knockout of *DNMT1*, *DNMT3B*, or both, to those of pharmacological manipulation. We performed extensive replicate experiments with multiple clones, cell lines, drug concentrations, and durations. The outcomes of this analysis yielded four major findings.

First, we were surprised to find that the effects of 5-aza-CdR on gene expression more closely resembled those of TSA than either of the somatic cell DNA methyltransferase knockouts, implying a converging mechanism for these agents. The effects on gene expression we observed were also remarkably consistent across dosage and duration of drug exposure and were largely independent of cell growth. Specifically, 5-aza-CdR effects were similar at one and five days. These data do not fit the conventional view that 5-aza-CdR acts on gene expression solely by incorporation into DNA during one cell division, followed by loss of methylation during subsequent rounds of replication. Rather, it suggests some form of active demethylation and/or perturbations of chromatin structure that affect gene expression. One possible mechanism might be an active demethylase in cells, as has been suggested by others (Keshet et al., 1986; Litt et al., 1997; Collas, 1998; Falk and Ernberg, 1999). Alternatively, both drugs could directly influence the stability of methylation and/or chromatin marks either directly or through their modifying proteins.

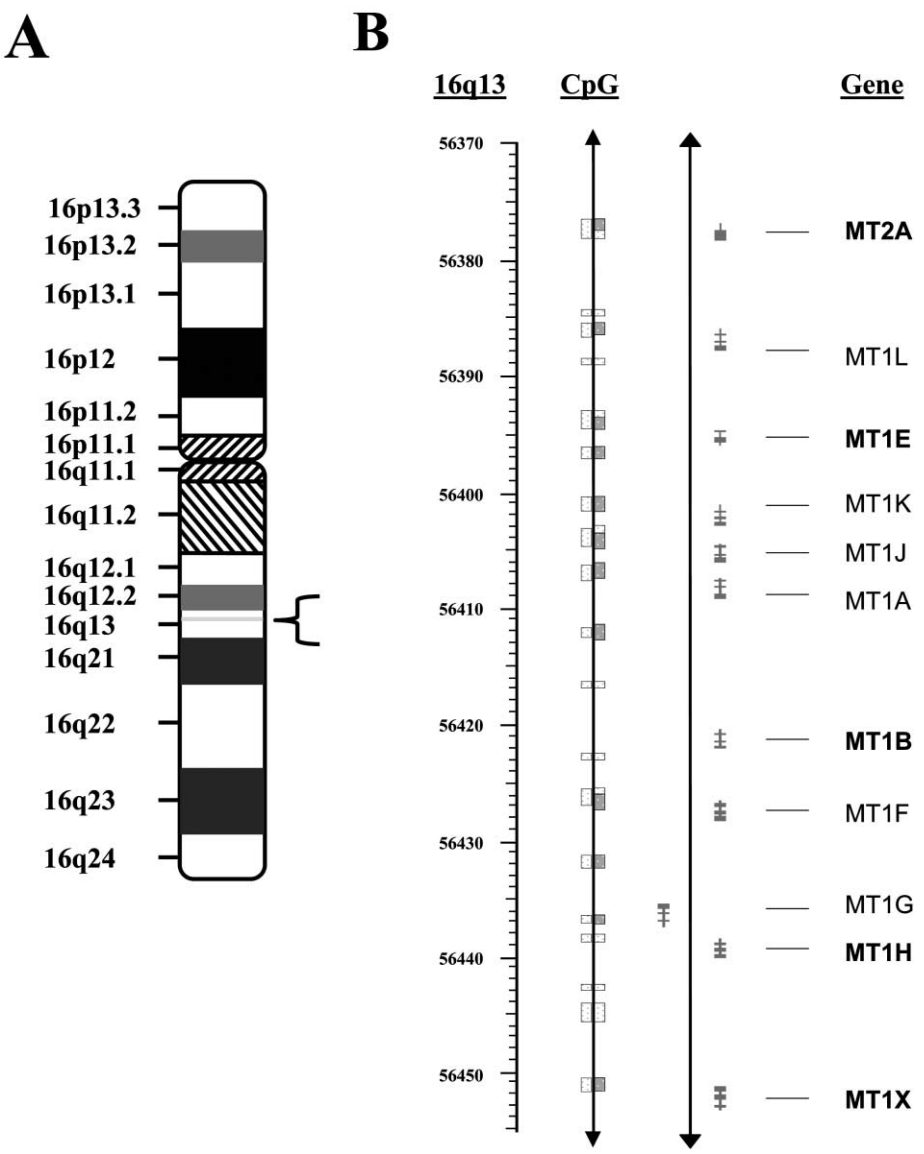

Figure 6. Metallothionein family genes constitute a cluster of differentially expressed genes

A: Diagram of chromosome 16 and the area of interest on 16q13.

B: Metallothionein genes upregulated in the DKO cells as well as other metallothionein genes in the chromosomal region of interest. Genes shown to be upregulated appear in bold, while the other metallothionein genes were not present on the microarray. Strict and relaxed CpG islands (as defined by NCBI) are denoted by gray and dotted boxes, respectively. Gene transcripts are shown with putative open reading frame as denoted by gray hash marks to the left of the NCBI abbreviation gene name.

Presently, the only other microarray study evaluating the effects of 5-aza-CdR or 5-aza-CdR and TSA on the modulation of gene expression did not compare the results to *DNMT* knockout cells or look for downregulated genes after exposure (Suzuki et al., 2002). In that study, a combined cDNA subtraction/microarray technique was used to increase the specificity of gene identification at the expense of sensitivity. In addition, the concentration of 5-aza-CdR (200–300 nM) was considerably lower than generally used to modulate gene expression, which may explain the small number of genes upregulated (74 genes) after exposure (Suzuki et al., 2002). Nevertheless, 70% of the genes identified in that study (which were also present on our gene set) were also shown to be upregulated following chemical exposure in our study. The difference between the two studies for the remaining 30% may be accounted for by the methodology of validation, semiquantitative versus real-time quantitative PCR in our study, and cell lines. Another important difference revealed by our epigenomic approach was the similarity between the effects of 5-aza-CdR and TSA, and the substantial difference between those from the effect of DNMT knockout, as described above. Suzuki et al. (2002) suggested that the effects of 5-aza-CdR were additive to those of TSA because of a distinct mechanism of action. However, the results presented here would argue that the pathways of action of these agents are overlapping.

The second major result is that the effects of the *DNMT1*$^{-/-}$ and *DNMT3B*$^{-/-}$ knockouts on gene expression overlapped each other in many cases, but also exhibited significant differences. *DNMT1*$^{-/-}$ altered total intracellular gene expression patterns to a much greater extent than that observed for the *DNMT3B*$^{-/-}$ knockout cells, suggesting that it is the dominant methyltransferase in this model system. In addition, the changes in gene expression in the DKO cells were less than those seen in *DNMT1*$^{-/-}$, suggesting a potential antagonistic mechanism between *DNMT1*- and *DNMT3B*-regulated genes.

Comparing the results from the present study to data on global methylation of *DNMT* knockout lines (Rhee et al., 2002), it appears that the extent of changes in global methylation were

not closely related to the specific changes in gene expression. Thus, we found substantial changes in gene expression even in single knockout lines, in spite of modest changes in global methylation. Furthermore, the pattern of gene expression was similar in our hands in the DKO cells, even though they underwent substantial global hypomethylation.

The specificity of *DNMT*-regulated gene expression is supported by a comparison of the data derived here to the results found in *DNMT1*$^{-/-}$ mouse fibroblasts. There was considerable similarity between the changes in expression of the genetic knockout that we observed, and a microarray analysis of *DNMT1*$^{-/-}$ mouse embryo fibroblasts (Jackson-Grusby et al., 2001), with substantial overlap in the patterns of gene expression (62%). In addition, the HCT116 *DNMT1*$^{-/-}$ cells showed increased doubling times and inherent apoptosis levels similar to those reported for the *DNMT1*$^{-/-}$ mouse fibroblasts cells (Jackson-Grusby et al., 2001), suggesting that *DNMT1* effects are generalized across cell types and species.

Third, a substantial fraction of genes were downregulated rather than upregulated after chemical and genetic manipulations, suggesting that hypomethylation *decreased* gene expression in these cases. Consistent with this hypothesis, analysis of the *APM2* gene promoter showed a decreased degree of methylation as the methyltransferase genes were deleted (Figure 5A), and this correlated with the degree of decrease in gene expression (Figure 2B). A potential mechanism for hypomethylation-mediated silencing is an insulator effect in chromatin. For example, CTCF, a chromatin insulator protein, binds to unmethylated GC-rich sequences, causing their silencing by separating enhancers from promoter elements (Fedoriw et al., 2004; Schoenherr et al., 2003), and consensus CTCF binding sites were found in all of the genes that exhibited downregulation (Figure 2B, Figure 5B). Thus, it will be important to investigate the role in cancer of the large number of normally methylated CpG islands that were recently identified (Strichman-Almashanu et al., 2002).

A surprising finding from the microarray analysis comparing and contrasting the effects of chemical and genetic modification of methyltransferase activity revealed a group of genes in which 5-Aza-CdR or TSA effects were *opposite* to those of *DNMT1* and/or *DNMT3B* knockout. This paradoxical effect on gene expression is most striking in *DNMT1*$^{-/-}$ cells exposed to 5-Aza-CdR or TSA (see Supplemental Figure S1 at http://www.cancercell.org/cgi/content/full/6/4/361/DC1/), as shown in regions IV and VII. For example, 11 genes were upregulated and 33 genes were downregulated paradoxically in the *DNMT1* knockout treated with 5-aza-CdR or TSA, respectively (see Supplemental Table S10). Similar results were observed for chemical treatment of the *DNMT3B*$^{-/-}$ cells. This reinforces the idea that pharmacological manipulation may not be equivalent to the genetic knockout of DNMT.

Finally, in at least one case, we identified a gene cluster belonging to the metallothionein family, spanning at least 76 kb, which showed coordinate regulation. These results suggest a novel mechanism involving methylation-induced regional chromosomal structural changes altering the expression of a class of related genes colocalized to a specific chromosomal region. While several members of this gene family have been shown to be regulated by methylation (Ghoshal et al., 2000; Majumder et al., 2002), other family member genes do not contain CpG islands in either the open reading frame or the upstream regulatory region. In addition, with more detailed gene arrays, there are likely to be additional such clusters, since the expression arrays were not designed a priori to identify them. Thus, an area for further research suggested by these experiments will be the identification of gene clusters that show coordinated changes in expression regulated by methylation or chromatin, and the elements responsible.

Experimental procedures

Cell culture and exposure to 5-aza-2′-Deoxycytidine and/or Trichostatin A

Multiple clones of the *DNMT1* knockout cell line (DNMT1$^{-/-}$), *DNMT3B* knockout cell line (DNMT3B$^{-/-}$), *DNMT1* and *DNMT3B* (double) knock out cell line (DKO), and parental colon cancer cell line (HCT116) were constructed as described (Rhee et al., 2002) and grown in McCoy's 5A medium (Invitrogen, Grand Island, NY). At least two cell clones were used in separate experiments to isolate RNA samples, and two microarrays were run on each RNA sample to account for cell line, RNA extraction, and microarray hybridization variability. Cell lines were passaged with about 50% confluence six hours before treatment. Cells were treated with designated doses of 5-aza-2′-deoxycytidine (5-aza-CdR; Sigma, St. Louis, MO), 100 ng/ml of Trichostatin A (TSA; Sigma, St. Louis, MO), or 5 mM of butyrate (Sigma, St. Louis, MO). The medium containing drugs was changed every day. Confluence of collected cells was not more than 80%.

RNA extraction

Total cellular RNA was isolated using ISOGEN (Maarssen, The Netherlands), according to the protocol supplied by the manufacturer. RNA was further purified using RNeasy Mini kit according to the manufacturer's recommendations (QIAGEN, Valencia, CA) with addition of DNase Digestion with RNase-free DNase set (QIAGEN, Valencia, CA). Purity was determined by gel analysis and spectrometrically. Reverse transcription and quantitative real-time PCR were carried out as described (Cui et al., 2001; Ravenel et al., 2001).

Probe labeling, microarray hybridization, and image and data analysis

Methodologies for the probe labeling reaction and microarray hybridization are previously described (Chuang et al., 2002). The microarrays used for this study contained 7,680 human cDNA clones and were prepared from the Research Genetics (Huntsville, AL) Named Genes set. These cDNA clones are enriched for known genes. All 7,680 cDNAs were spotted onto poly-L-lysine-coated slides (NCI ROSP 8k Human Array) using an OmniGrid arrayer (GeneMachines, San Carlos, CA) (Eisen and Brown, 1999). Microarrays were scanned at 10 μm resolution on a GenePix 4000A scanner (Axon Instruments, Inc., Foster City, CA). The Cy5- and the Cy3-labeled cDNA samples were scanned at 635 nm and 532 nm, respectively. The resulting TIFF images were analyzed by GenePix Pro 3.0 software (Axon Instruments, Inc., Foster City, CA).

The ratios of the sample intensity to the reference intensity (green [Cy3]/red [Cy5]) for all targets were determined. Since a normal distribution could not be applied to all components of the data set, a Mann-Whitney test was used to ascertain statistical significance among microarray replicates (Troyanskaya et al., 2002). Well fluorescence was corrected for background fluorescence, and ratios of intensity were established relative to appropriate controls. We selected a 1.5-fold threshold in differences because the multiple repeats in our experimental scheme increase the likelihood of statistical reliability. Three additional analytical methods were employed to validate statistical integrity: class comparison, class prediction, and false discovery, all preformed at $p = 0.05$ to validate statistical integrity (See Supplemental Tables S2 and S3 at http://www.cancercell.org/cgi/content/full/6/4/361/DC1/).

In some cases, additional genes were included so that the hierarchal cluster map would show novel clusters of important genes. Importantly, we do not refer to individual genes as only increased by 1.5-fold, but rather to gene clusters based on the multiple experimental conditions. In most cases, at least one of the conditions had increases greater than 2-fold or decreases less than 2-fold. Pearson's moment correlation coefficients ($r\rho$) were calculated from fluorescent ratio data and relate the overall similarity in gene

expression patterns between the two data sets under comparison. Values of $r\rho$ range from -1 (no correlation) to 1 (complete correlation).

Proliferation and apoptosis assays

For proliferation assays, cells were seeded at a density of 2×10^4 cells per 35 mm dish and returned to a humidified 37°C, 5% CO_2 incubator for growth. Designated samples contained 5-aza-CdR at 1 or 10 μM concentrations in the media. For the following days, three plates from each treatment condition were trypsinized and quantified via a Z2 Counter (Beckman-Coulter, Fullerton, CA), with fresh medium added daily. Growth curves were plotted as the mean number of cells per dish as a function of time (d).

Assays for apoptosis detection and measurement were performed according to the manufacturer's instructions (Annexin V-FITC Apoptosis Detection Kit, Oncogene Research, San Diego, CA). Data from 10,000 events were collected on a FACSCalibur cytometer (BD Immunocytometry, Fullerton, CA) and analyzed using CellQuest/ModFit software. Results for early and late apoptosis were summed to calculate the total amount of apoptosis from two time points. Samples treated with camptothecin (4 μM, 42 hr; Sigma, St. Louis, MO) were used as positive controls.

Bisulfite sequencing analysis

The CpG island located on the promoter and 5′ of the *APM2* gene was obtained from the University of California, Santa Cruz Genome Bioinformatics Site (http://www.genome.ucsc.edu) and corresponds to GenBank nucleotides 2417–3096 (NCBI Accession: AL136982). After bisulfite treatment, DNA methylation was analyzed by PCR sequencing using primers 5′-GAAG TTATGGTAAGTAAGGGTTTGTAG-3′ and 5′-TCCCTATCCTAAACCTTCAC CCTCTCCTA-3′, followed by 5′-TGTAGGATTTGAAGTAATAGGTG-3′ and 5′-CCAACATAACCTCCTTAAAAAAACTCC-3′, both annealing at 55°C. Other conditions are as described previously (Cui et al., 2003).

Genomic location analysis: Apparent clusters

This approach is described in some detail, as this analysis represents the first location cluster of differentially expressed genes identified. This was developed by L.Y. and P.J.M. at CIT/NIH, and the method has not been reported previously. The method involves finding a dense cluster, or closely spaced set of coregulated genes, and determines the statistical significance of such findings. The method is completely defined in the Supplemental Experimental Procedures at http://www.cancercell.org/cgi/content/full/6/4/361/DC1/. Using numerical simulation with 10,000 iterations, the probability of observing a cluster with the same or more genes in the same or smaller span of DNA sequence, within a chromosome of the same length, containing the same number of genes as the found cluster, is determined. The method correctly accounts for the nonuniform spacing of genes within chromosomes, and the multiple comparisons inherent in searching for clusters of an unknown number of genes (see Supplemental Experimental Procedures). The unaveraged, raw gene expression data are available as Supplemental Tables S4, S6, S7, and S9.

Acknowledgments

We thank Ina Rhee and Bert Vogelstein for the HCT116 knockout cell lines. This work was supported by grants CA65145 (A.P.F.), CA72602 (D.G.), and CA75556 (D.G.) from the National Institutes of Health.

Received: January 23, 2004
Revised: April 27, 2004
Accepted: August 3, 2004
Published: October 18, 2004

References

Bell, A.C., West, A.G., and Felsenfeld, G. (1999). The protein CTCF is required for the enhancer blocking activity of vertebrate insulators. Cell *98*, 387–396.

Bell, A.C., and Felsenfeld, G. (2000). Methylation of a CTCF-dependent boundary controls imprinted expression of the Igf2 gene. Nature *405*, 482–485.

Bestor, T.H. (2000). The DNA methyltransferases of mammals. Hum. Mol. Genet. *9*, 2395–2402.

Carvalho, R., Kayademir, T., Soares, P., Canedo, P., Sousa, S., Oliveira, C., Leistenschneider, P., Seruca, R., Gott, P., Blin, N., et al. (2002). Loss of heterozygosity and promoter methylation, but not mutation, may underlie loss of TFF1 in gastric carcinoma. Lab. Invest. *82*, 1319–1326.

Chuang, Y.Y.E., Chen, Y., Gadisetti, C., Chandramouli, V.R., Cook, J.A., Coffin, D., Tsai, M.H., DeGraff, W., Yan, H., Zhao, S., et al. (2002). Gene expression after treatment with hydrogen peroxide, menadione, or t-butyl hydroperoxide in breast cancer cells. Cancer Res. *62*, 6246–6254.

Collas, P. (1998). Modulation of plasmid DNA methylation and expression in zebrafish embryos. Nucleic Acids Res. *26*, 4454–4461.

Cui, H., Niemitz, E.L., Ravenel, J.D., Onyango, P., Brandenburg, S.A., Lobanenkov, V.V., and Feinberg, A.P. (2001). Loss of imprinting of insulin-like growth factor-II in Wilms' tumor commonly involves altered methylation but not mutations of CTCF or its binding site. Cancer Res. *61*, 4947–4950.

Cui, H., Cruz-Correa, M., Giardiello, F.M., Hutcheon, D.F., Kafonek, D.R., Brandenburg, S., Wu, Y., He, X., Powe, N.R., and Feinberg, A.P. (2003). Loss of *IGF2* imprinting: A potential marker of colorectal cancer risk. Science *299*, 1753–1755.

Egger, G., Liang, G., Aparicio, A., and Jones, P.A. (2004). Epigenetics in human disease and prospects for epigenetic therapy. Nature *429*, 457–463.

Eisen, M.B., and Brown, P.O. (1999). DNA arrays for analysis of gene expression. Methods Enzymol. *303*, 179–205.

Falk, K.I., and Ernberg, I. (1999). Demethylation of the Epstein-barr virus origin of lytic replication and of the immediate early gene *BZLF1* is DNA replication independent. Brief report. Arch. Virol. *144*, 2219–2227.

Fedoriw, A.M., Stein, P., Svoboda, P., Schultz, R.M., and Bartolomei, M.S. (2004). Transgenic RNAi reveals essential function for CTCF in H19 gene imprinting. Science *303*, 238–240.

Feinberg, A.P., and Tycko, T. (2004). Timeline: The history of cancer epigenetics. Nat. Rev. Cancer *4*, 1–11.

Feinberg, A.P., and Vogelstein, B. (1983). Hypomethylation distinguishes genes of some human cancers from their normal counterparts. Nature *301*, 89–92.

Furstenberger, G., and Senn, H.J. (2002). Insulin-like growth factors and cancer. Lancet Oncol. *3*, 298–302.

Ghoshal, K., Majumder, S., Li, Z., Dong, X., and Jacob, S.T. (2000). Suppression of metallothionein gene expression in a rat hepatoma because of promoter-specific DNA methylation. J. Biol. Chem. *275*, 539–547.

Goelz, S.E., Vogelstein, B., Hamilton, S.R., and Feinberg, A.P. (1985). Hypomethylation of DNA from benign and malignant human colon neoplasms. Science *228*, 187–190.

Greger, V., Passarge, E., Hopping, W., Messmer, E., and Horsthemke, B. (1989). Epigenetic changes may contribute to the formation and spontaneous regression of retinoblastoma. Hum. Genet. *83*, 155–158.

Guillaudeux, T., Gomez, E., Onno, M., Drenou, B., Segretain, D., Alberti, S., Lejeune, H., Fauchet, R., Jegou, B., and Le Bouteiller, P. (1996). Expression of *HLA class I* genes in meiotic and post-meiotic human spermatogenic cells. Biol. Reprod. *55*, 99–110.

Hark, A.T., Schoenherr, C.J., Katz, D.J., Ingram, R.S., Levorse, J.M., and Tilghman, S.M. (2000). CTCF mediates methylation-sensitive enhancer-blocking activity at the *H19/Igf2* locus. Nature *405*, 486–489.

Holmgren, C., Kanduri, C., Dell, G., Ward, A., Mukhopadhya, R., Kanduri, M., Lobanenkov, V., and Ohlsson, R. (2001). CpG methylation regulates the *Igf2/H19* insulator. Curr. Biol. *11*, 1128–1130.

Jackson-Grusby, L., Beard, C., Possemato, R., Tudor, M., Fambrough, D., Csankovszki, G., Dausman, J., Lee, P., Wilson, C., Lander, E., and Jaenisch, R. (2001). Loss of genomic methylation causes p53-dependent apoptosis and epigenetic deregulation. Nat. Genet. *27*, 31–39.

Keshet, I., Lieman-Hurwitz, J., and Cedar, H. (1986). DNA methylation affects the formation of active chromatin. Cell *44*, 535–543.

Lengauer, C., Kinzler, K.W., and Vogelstein, B. (1998). Genetic instabilities in human cancers. Nature *396*, 643–649.

Litt, M.D., Hansen, R.S., Hornstra, I.K., Gartler, S.M., and Yang, T.P. (1997). 5-Azadeoxycytidine-induced chromatin remodeling of the inactive X-linked *HPRT* gene promoter occurs prior to transcription factor binding and gene reactivation. J. Biol. Chem. *272*, 14921–14926.

Majumder, S., Ghoshal, K., Datta, J., Bai, S., Dong, X., Quan, N., Plass, C., and Jacob, S.T. (2002). Role of de novo DNA methyltransferases and methyl CpG-binding proteins in gene silencing in a rat hepatoma. J. Biol. Chem. *277*, 16048–16058.

Nie, Y., Yang, G., Song, Y., Zhao, X., So, C., Liao, J., Wang, L.D., and Yang, C.S. (2001). DNA hypermethylation is a mechanism for loss of expression of the *HLA class I* genes in human esophageal squamous cell carcinomas. Carcinogenesis *22*, 1615–1623.

Ohtani-Fujita, N., Fujita, T., Aoike, A., Osifchin, N.E., Robbins, P.D., and Sakai, T. (1993). CpG methylation inactivates the promoter activity of the human retinoblastoma tumor-suppressor gene. Oncogene *8*, 1063–1067.

Paz, M.F., Wei, S., Cigudosa, J.C., Rodriguez-Perales, S., Peinado, M.A., Huang, T.H., and Esteller, M. (2003). Genetic unmasking of epigenetically silenced tumor suppressor genes in colon cancer cells deficient in DNA methyltransferases. Hum. Mol. Genet. *121*, 2209–2219.

Ravenel, J.D., Broman, K.W., Perlman, E.J., Niemitz, E.L., Jayawardena, T.M., Bell, D.W., Haber, D.A., Uejima, H., and Feinberg, A.P. (2001). Loss of imprinting of insulin-like growth factor-II (*IGF2*) gene in distinguishing specific biologic subtypes of Wilms tumor. J. Natl. Cancer Inst. *93*, 1698–1703.

Rhee, I., Jair, K.W., Yen, R.W., Lengauer, C., Herman, J.G., Kinzler, K.W., Vogelstein, B., Baylin, S.B., and Schuebel, K.E. (2000). CpG methylation is maintained in human cancer cells lacking *DNMT1*. Nature *404*, 1003–1007.

Rhee, I., Bachman, K.E., Park, B.H., Jair, K.W., Yen, R.W., Schuebel, K.E., Cui, H., Feinberg, A.P., Lengauer, C., Kinzler, K.W., et al. (2002). *DNMT1* and *DNMT3b* cooperate to silence genes in human cancer cells. Nature *416*, 552–556.

Robertson, K.D. (2001). DNA methylation, methyltransferases, and cancer. Oncogene *20*, 3139–3155.

Sakai, T., Toguchida, J., Ohtani, N., Yandell, D.W., Rapaport, J.M., and Dryja, T.P. (1991). Allele-specific hypermethylation of the retinoblastoma tumor-suppressor gene. Am. J. Hum. Genet. *48*, 880–888.

Schmid, M., Haaf, T., and Grunert, D. (1984). 5-azacytidine-induced under-condensations in human chromosomes. Hum. Genet. *67*, 257–263.

Schoenherr, C.J., Levorse, J.M., and Tilghman, S.M. (2003). CTCF maintains differential methylation at the *Igf2*/*H19* locus. Nat. Genet. *33*, 66–69.

Storks, P.J. (2003). Does Rap1 deserve a bad Rap? Trends Biochem. Sci. *28*, 267–275.

Strichman-Almashanu, L.Z., Lee, R.S., Onyango, P.O., Perlman, E., Flam, F., Frieman, M.B., and Feinberg, A.P. (2002). A genome-wide screen for normally methylated human CpG islands that can identify novel imprinted genes. Genome Res. *12*, 543–554.

Suzuki, H., Gabrielson, E., Chen, W., Anbazhagan, R., van Engeland, M., Weijenberg, M.P., Herman, J.G., and Baylin, S.B. (2002). A genomic screen for genes upregulated by demethylation and histone deacetylase inhibition in human colorectal cancer. Nat. Genet. *31*, 141–149.

Tamaru, H., and Selker, E.U. (2001). A histone H3 methyltransferase controls DNA methylation in Neurospora crassa. Nature *414*, 277–283.

Tang, J., Kao, P.N., and Herschman, H.R. (2000). Protein-arginine methyltransferase I, the predominant protein-arginine methyltransferase in cells, interacts with and is regulated by interleukin enhancer-binding factor 3. J. Biol. Chem. *275*, 19866–19876.

Troyanskaya, O.G., Garber, M.E., Brown, P.O., Botstein, D., and Altman, R.B. (2002). Nonparametric methods for identifying differentially expressed genes in microarray data. Bioinformatics *18*, 1454–1461.

Ulleras, E., Miller, S.J., Adam, G.I., Kanduri, C., Wilcock, A.C., and Franklin, G.C. (2001). Inhibition of histone deacetylase activity causes cell type-specific induction of the *PDGF-B* promoter only in the absence of activation by its enhancer. Exp. Cell Res. *270*, 188–198.